Biointerface Research in Applied Chemistry
Open-Access Journal (ISSN: 2069-5837)

Article
Volume 16, Issue 2, 2026, 62
https://doi.org/10.33263/BRIAC16.062

Synthesis and Characterization of the BEAC6ND4 Ionophore from *p-t*-Butylcalix[6]arene Carboxylic Acid

Nasriadi Dali [1,*], Armadi Chairunnas [2], Arnadi Chairunnas [3], Hilda Ayu Melvi Amalia [4], Sri Ayu Andini Puspita Sari [5]

[1] Department of Chemistry, Faculty of Mathematics and Natural Sciences, Halu Oleo University, Kendari 93232 - Southeast Sulawesi, Indonesia; nasriadidali@ymail.com (N.D.); nasriadi.dali@uho.ac.id;
[2] Regional Research and Innovation Agency of Southeast Sulawesi Province, Kendari 93121 - Southeast Sulawesi, Indonesia; armadisajami@gmail.com (A.C.); armadi.hairunnas@sultraprov.go.id;
[3] Department of Accounting, Faculty of Social Sciences and Economics, Sembilanbelas November University, Kolaka 93517 - Southeast Sulawesi, Indonesia; arnadichairunnas@gmail.com (A.C.); arnadi.chairunnas@usn.ac.id;
[4] Study Program of Tadris Biology, Faculty of Tarbiyah and Teacher Training, Institut Agama Islam Negeri (IAIN), Kendari 93563 - Southeast Sulawesi, Indonesia; hildaayumelvi@gmail.com (H.A.M.A.); hildaayumelvi@iainkendari.ac.id;
[5] Department of Public Health, Faculty of Public Health, Halu Oleo University, Kendari 93232 - Southeast Sulawesi, Indonesia; sriayuandinip@gmail.com (S.A.A.P.S.); sriayu.andini@uho.ac.id;
* Correspondence: nasriadidali@ymail.com;

Received: 9.03.2025; Accepted: 14.11.2025; Published: 15.04.2026

Abstract: *p-t*-Butylcalix[6]arene carboxylic acid has been effectively converted into the BEAC6ND4 ionophore. The synthetic procedure produced the BEAC4ND4 ionophore in two stages. *p-t*-Butylcalix[6]arene carboxylic acid and thionyl chloride undergo a chlorination reaction in a dry benzene solvent as the initial step. *p-t*-Butylcalix[6]arene acyl chloride is the end product of the chlorination procedure. It is a light brown viscous liquid with a randomness of 74.88% and TLC (SiO_2, CH_3OH: CH_2Cl_2 = 1: 1 v/v, R_f = 0.69). The amidation reaction between ethyl 2-aminoacetate and *p-t*-butylcalix[6]arene acyl chloride in a dry tetrahydrofuran solvent is the second step. The *p-t*-butylcalix[6]arene ethylesteramide, also known as the BEAC6ND4 ionophore, is the end product of the amidation reaction. It is a white solid with a randomness of 65.30%, a melting point of 345-347°C, and TLC (SiO_2, CH_3OH: CH_2Cl_2 = 1: 1 v/v, R_f = 0.79).

Keywords: BEAC6ND4 ionophore; chlorination; amidation; calix[6]arene; carboxylic acid.

1. Introduction

Only a small amount of calix[4]-and-[6]arenes dissolve in organic solvents. By altering the calix[4]-and-[6]arenes' top and lower rims, the solubility can be improved. The *p-t*-butylcalix[4]-and-[6]arenes can become more soluble in water and dichloromethane [1] by altering the lower rim with thioamide. By adding sulfonates to the top rim, calix[4]-and-[6]arenes become more soluble in methanol. In addition to making calix more soluble, alteration can enhance its qualities and broaden its range of uses calix[4]-and [6] arene. Lower rim modifications using ethers, esters, ketones, carboxylic acids, amides, and crown ethers [1] can result in ionophores with highly selective binding capabilities for Na^+, Cs^+, Ca^{2+}, Mg^{2+} [2], and Fe^{3+}, Ni^{2+}, Cr^{2+} [3] cations.

The most common and well-researched functionalization is the hydroxyl groups on the bottom rim of calix[4]-and-[6]arenes being functionalized by esterification and etherification processes. Researchers have documented group modification on the lower rim of calix[4]-and-[6]arenes, such as tetra(carboxylic)calix[4]arene [3], tri(ethoxycarbonyl methoxy)tri(hydroxy)calix[6]arene [4], hexa(ethylester)calix[6]arene [5], tetrakis(ethoxycarbonylmethoxy)calix[4]arene [6], tetra(propenyltetraester)calix[4]arene [7], and tetra(propenyltetracarboxylicacid)calix[4]arene [7].

By altering *p*-*t*-butyl with additional groups, the upper rim of calix[4]-and-[6]arenes can be functionalized. A Friedel-Crafts dealkylation procedure can be used to eliminate the *p*-*t*-butyl group from calix[4]-and-[6]arenes [8]. Moreover, electrophilic aromatic substitution processes may bind the new group to the *para* position. For instance, *p*-H-calix[4]arene is produced by the Friedel-Crafts dealkylation process of *p*-*t*-butylcalix[4]arene. The *para*-substituted calix[4]arenes with different *para*-substituents are produced via electrophilic aromatic substitution processes of *p*-H-calix[4]arene.

The *p*-H-calix[4]-and-[6]arenes undergo the Mannich reaction with formaldehyde and dimethylamine to produce *p*-aminomethylcalix[4]-and-[6]arenes, which can then react with MeI to produce the equivalent quaternary ammonium compounds. The *p*-Nu-methyl calix[4]-and-[6]arenes are produced when a nucleophile attacks the ammonium salts. In the presence of base, *p*-H-calix[4]-and-[6]arenes are alkylated with allyl bromide to produce tetraallyl ether, which then goes through the Claisen rearrangement to produce *p*-allylcalix[4]-and-[6]arenes [9]. Therefore, one, two, three, or four substituents (same or different) can be added to the *para*-positions of calix[4]arenes by combining the lower rim modification reactions with certain protection-deprotection techniques.

Ionophores can be produced by altering the functional groups of the calix[4]-and-[6]arenes' upper and lower rims [4,6,8]. The bottom rim's OH group of calix[4]-and-[6]arenes undergoes modification events with ethylester to yield the ionophores BEC4ND1 [3] and BEC6ND1 [2]. The lower rim's ethylester group of calix[4]-and-[6]arenes undergoes modification events with carboxylic acid to yield the ionophores BCAC4ND2 [10] and BCAC6ND2 [11]. Modification reactions of the lower rim's carboxylic acid group of calix[4]arenes with ethylesteramide produce BEAC4ND4 ionophore [12]. An ionophore that is specific to the cations of Rb, Sr, Cs, alkali metals, and alkaline earth metals is produced by modification reactions of the upper rim's *t*-butyl group with a tetramer or hexamer [13].

In both analytical and industrial chemistry, metal ion separation is a crucial process. If metal ions are to be purified or recovered from wastewater, they must be selectively separated. One separation method that can be used in industrial wastewater treatment is liquid membrane transport. In this method, metal ions are transported from a source phase to a target phase through an organic liquid membrane containing ion-carrying molecules or ionophores. This method relies heavily on the stability of the complex between the metal ion and the ionophore. The type of donor atom (active group), ring size, and the length of the hydrophobic branch of the ionophore determine the stability of this complex. Therefore, ionophores in liquid membranes significantly influence the transport efficiency and selectivity of various extraction methods. Calix[n]arene and its derivatives are macrocyclic compounds with great potential for use as ionophores.

The compound *p*-*t*-butyl(carboxymethoxy)calix[6]arene is one of the calix derivatives that has been successfully synthesized [11]. In this study, we modified the structure of this compound by substituting the carboxylic acid group (COOH) below the ring with an ethyl ester

amide group ($CONHCH_2COOCH_2CH_3$). This was designed to increase its reactivity, selectivity, and effectiveness as an ionophore when binding metal ions to each other. Because basic O and N atoms can donate electrons to form coordination bonds with metal ions, especially metal ions that are classified as soft acids, the presence of basic O and N atoms in the amide group can make the binding of metal ions more effective. Consequently, the aim of this study is to synthesize the BEAC6ND4 ionophore from carboxylic acid *p-t*-butylcalix[6]arene. It is expected that the presence of the BEAC6ND4 ionophore, as a new compound, enables ion carrier molecules to separate metal ions using the liquid membrane transport method.

2. Materials and Methods

2.1. Apparatus and materials.

A rotary vacuum evaporator (BUCHI Rotavapor™ series R-300), a digital melting point apparatus (Electrothermal series IA9100), a desiccator, an analytical balance (Explorer Ohaus), a measuring cup (Pyrex), a chemical beaker (Pyrex), a chamber, ball coolers, thermometers (100°C), heating mantles, funnels, and a set of reflux devices comprising a 100 mL three-neck round bottom flask are among the instruments utilized. The FTIR Shimadzu series Prestige-21 and the FTNMR Jeol series JNM-MY500 are the spectrometers that are utilized.

The raw materials, *p-t*-butylcalix[6]arene carboxylic acid (synthesized), benzene p.a (Merck), thionyl chloride p.a (Merck), pyridine p.a (Merck), tetrahydrofuran (THF) p.a (Merck), ethyl ester amines p.a (Merck), triethylamine p.a (Merck), methanol p.a (Merck), dichloromethane p.a (Merck), anhydrous sodium sulfate (Na_2SO_4) p.a (Merck), aquabidest (Onelab Waterone), nitrogen gas (commercial), and TLC plate are the materials utilized.

2.2. Synthesis of the BEAC6ND4 ionophore.

Thionyl chloride (5 mL) and three drops of pyridine were added to 25 mL of dry benzene containing *p-t*-butylcalix[6]arene carboxylic acid (0.44 g, 0.5 mmol). For eight hours at room temperature, the mixture was agitated and refluxed under nitrogen. To regulate the reaction outcomes, the mixture was subjected to TLC testing every two hours. Distillation was used to separate the *p-t*-butylcalix[6]arene acyl chloride solution (bp. 182°C) from the thionyl chloride solution (bp. 74.6°C). Since the *p-t*-butylcalix[6]arene acyl chloride solution is unstable, it is employed right away without additional purification [14-17].

At atmospheric conditions, nitrogen, a solution of ethyl 2-aminoacetate (0.21 mL, 1.8328 mmol) and trimethylamine (0.21 mL, 2.227 mmol) in dry THF (10 mL) was mixed dropwise with a solution of *p-t*-butylcalix[6]arene acyl chloride (0.23 g, 0.2409 mmol) in dry THF (5 mL). Nitrogen gas was added to the mixture and stirred with a magnetic stirrer for 24 hours at room temperature. To monitor reaction outcomes, the mixture was analyzed by TLC every 8 hours. In addition, the mixture was filtered, and the rotavapor was used to concentrate the filtrate at 66°C. After dissolving the residue in 10 mL of dichloromethane, the mixture was rinsed with 10 mL of cold water (-5°C). Additionally, anhydrous Na_2SO_4 was used to dry the solution. After filtering the product solution, the rotavapor was used to evaporate the solvent at 39.6°C. Methanol and dichloromethane were used to recrystallize the crystals that had formed. The BEAC6ND4 ionophore is the white solid that is produced. Additionally, the desiccator is used to dry the BEAC6ND4 ionophore before it is characterized using TLC,

melting point, FTIR, and FTNMR (^{1}H, ^{13}C). The ^{1}H-NMR and ^{13}C-NMR experiments were performed at 408°C and 406.5°C, respectively.

2.3. Determination of the BEAC6ND4 ionophore structure.

FTIR and FTNMR 1-D (^{1}H, ^{13}C) are two spectroscopic methods that were used to determine the structure of the BEAC6ND4 ionophore. The BEAC6ND4 ionophore's physical characteristics include a white solid with a randomness of 65.30%; mp 345-347°C; and TLC (SiO_2, CH_3OH: CH_2Cl_2 = 1: 1 v/v, R_f = 0.79). The BEAC6ND4 ionophore's FTIR and FTNMR (^{1}H, ^{13}C) spectra data are shown in the description that follows. FTIR (KBr) ν_{maks} (cm^{-1}): 1749.44 (esters C=O stretch), 1114.86 (C-O-C stretch in dialkyl ethers), 1242.16 (C-O-C stretch in alkyl aryl ethers), 1066.64 (R-C-O stretch in alkyl aryl ethers), 3055.24 and 3024.38 (CH stretch of unsaturated aromatic), 1633.71 (aromatic C=C stretch), 1201.65 (aromatic C-O stretch), 873.75 and 723.31 (CH out-of-plane deformation of disubstituted *para* aromatic), 3446.79 and 3147.83 (NH stretch of secondary amides), 1645.28 (C=O stretch of secondary amides) (amide I band), 1483.26 (C-N stretch of secondary amides) (amide II band), 2958.8, 2906.73, and 2866.22 (CH stretch of $(CH_3)_3C$ saturated aliphatic), 1394.53 (CH stretch of CH_3 aliphatic), and 1458.18 (CH stretch of CH_2 aliphatic); **^{1}H**-NMR (500 MHz, $CDCl_3$) δ_H (ppm): 7.1275 [(s, 1**H**) (Ar**H**-34/36)], 4.3157 [(s, 2**H**) (C**H**$_2$O-2")], 5.9311 [(s, 1**H**) (N**H**-1^)], 2.5315 [(s, 2**H**) (C**H**$_2$NH-1$^{\#}$)], 3.0216 [(q, 2**H**, *J* = 6.7 Hz) (OC**H**$_2$CH$_3$-1*)], 1.4566 [(t, 3**H**, *J* = 6.7 Hz) (OCH$_2$C**H**$_3$-2*)], 4.2214 [(d, 2**H**, *J* = 12.9 Hz) (ArC**H**$_2$Ar-32)], 3.7415 [(d, 2**H**, *J* = 12.9 Hz) (ArC**H**$_2$Ar-2$_{a,b}$)], 1.2426 [(s, 9**H**) (C(C**H**$_3$)$_3$-2')]; **^{13}C**-NMR (500 MHz, $CDCl_3$) δ_C (ppm): 172.2135 [(**C**=O amides) (**C**-1")], 42.3405 [**C**H$_2$ amides) (**C**-1$^{\#}$)], 170.3562 [(**C**=O esters) (**C**-2$^{\#}$)], 62.6373 [(**C**H$_2$ esters) (**C**-1*)], 11.3696 [(**C**H$_3$ esters) (**C**-2*)], 146.7315 [(**C**-O aryl) (**C**-37)], 144.4292 [(**C**-*para* aryl) (**C**-35)], 127.0885 [(**C**-*ortho* aryl) (**C**-1/**C**-33)], 126.3255 [(**C**-*meta* aryl) (**C**-34/**C**-36)], 73.4327 [(ArO**C**H$_2$-) (**C**-2")], 34.1757 [(**C**(CH$_3$)$_3$) (**C**-1')], 33.1742 [(Ar**C**H$_2$Ar) (**C**-2/**C**-32)], and 31.6576 [(C(**C**H$_3$)$_3$) (**C**-2')]. The position of the chemical shift value of ^{1}H and **^{13}C**-NMR in the carbon framework of the BEAC6ND4 ionophore can be seen in Figure 1.

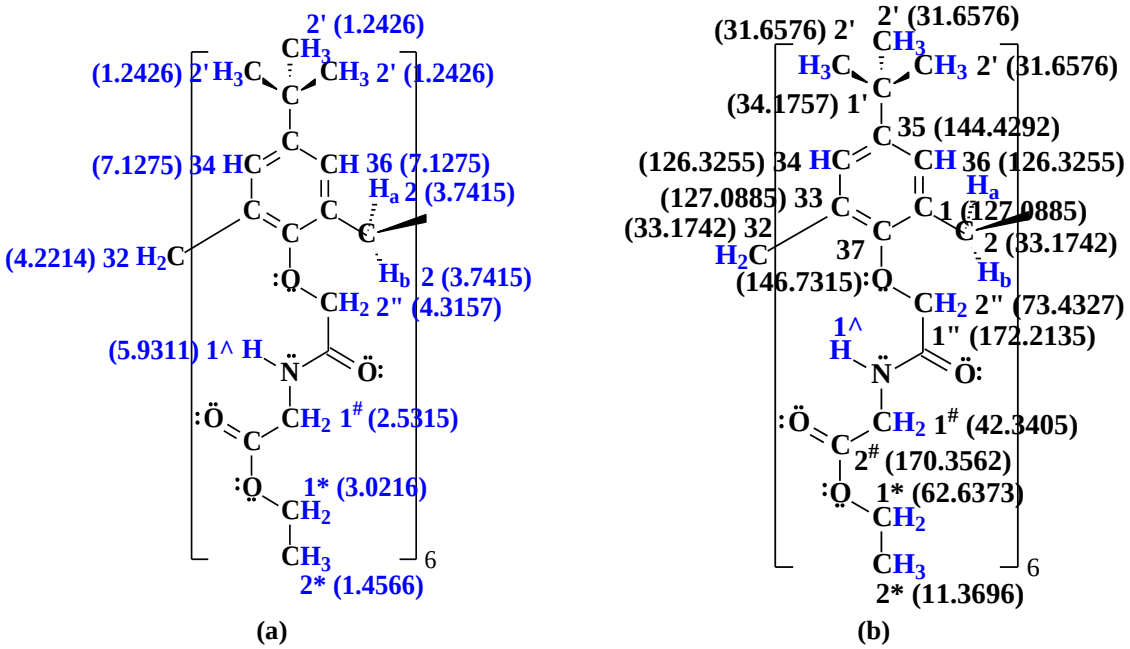

Figure 1. The location of the **(a)** ^{1}H-NMR; **(b)** ^{13}C-NMR chemical shift values within the BEAC6ND4 ionophore's carbon framework.

3. Results and Discussion

3.1. Synthesis of the BEAC6ND4 ionophore.

3.1.1. Chlorination reaction.

The chlorination reaction of *p-t*-butylcalix[6]arene carboxylic acid with thionyl chloride in dry benzene is the initial stage of the production procedure of the BEAC6ND4 ionophore (Figure 2). Using TLC (SiO_2, CH_3OH: CH_2Cl_2 = 1: 1 v/v, R_f = 0.69), the *p-t*-butylcalix[6]arene acyl chloride was produced as a light brown viscous liquid with a yield of 74.88%. The synthesis product's R_f value (0.69) is less than the reactant's R_f value (0.93) (Figure 3). When the synthesis product is more polar than the reactant, this is consistent with expectations. Due to its strong reactivity with water vapor [18-20], *p-t*-butylcalix[6]arene acyl chloride is not investigated spectroscopically.

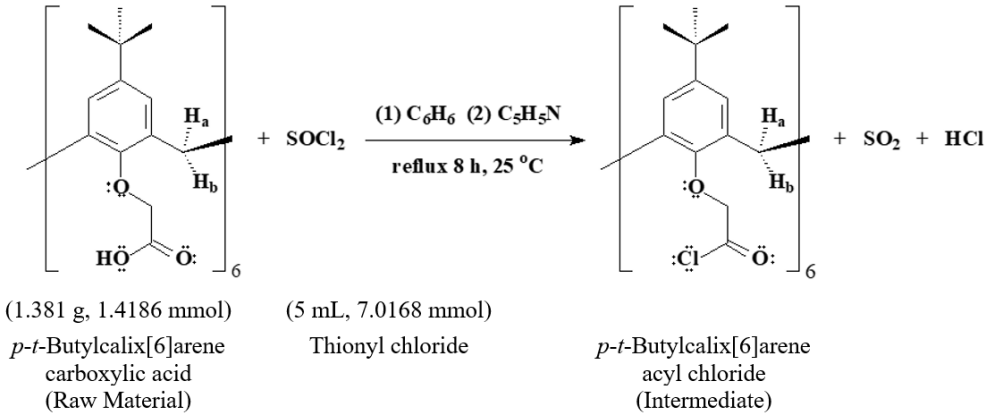

Figure 2. The *p-t*-butylcalix[6]arene carboxylic acid and thionyl chloride undergo a chlorination reaction to produce *p-t*-butylcalix[6]arene acyl chloride.

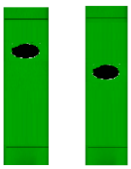

Figure 3. Results of the TLC (SiO_2, CH_3OH: CH_2Cl_2 = 1 : 1 v/v) test: **(a)** Carboxylic acid of *p-t*-butylcalix[6]arene (R_f = 0.93); **(b)** Acyl chloride of *p-t*-butylcalix[6]arene (R_f = 0.69).

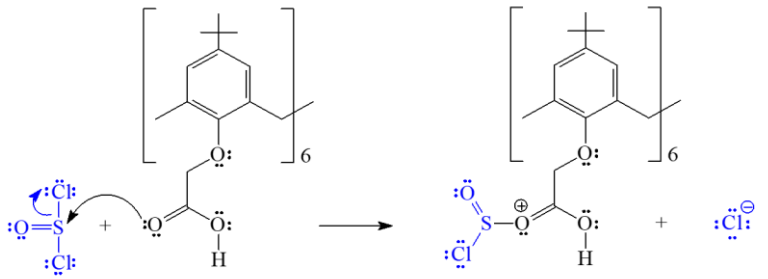

Figure 4. The reaction of *p-t*-butylcalix[6]arene carboxylic acid and thionyl chloride to form acyl chlorosulfite calix[6]arene ion and chloride ion.

Figure 2 shows the synthesis reaction of *p-t*-butylcalix[6]arene acyl chloride from *p-t*-butylcalix[6]arene carboxylic acid. The reaction mechanism of acyl chloride synthesis involves nucleophilic substitution by chloride ion on acyl chlorosulfite (a reactive intermediate). In the initial step, thionyl chloride reacts with *p-t*-butylcalix[6]arene hexacarboxylate to form acyl chlorosulfite calix[6]arene ion and chloride ion (Figure 4).

Next, the chloride ion acts as a nucleophile (S_N2) and attacks the acyl carbon (electrophile) of the chlorosulfite acyl ion, so that the chloride ion replaces the chlorosulfite ion to form *p-t*-butylcalix[6]arene acyl chloride (Figure 5).

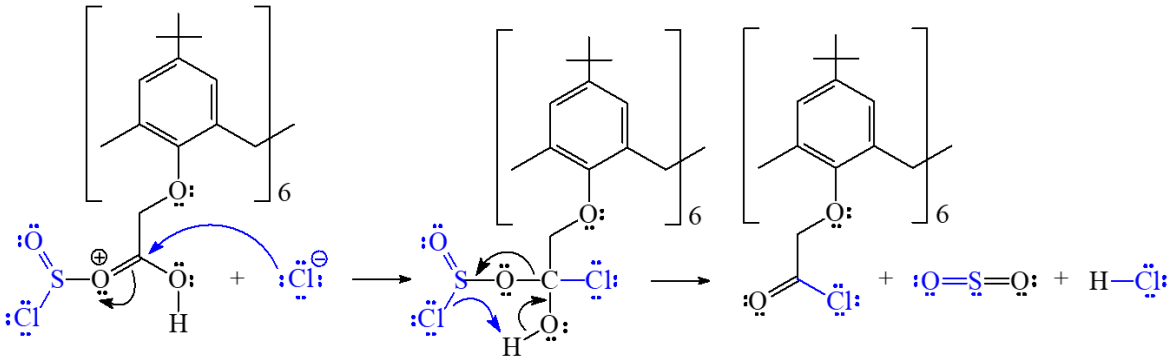

Figure 5. The reaction of acyl chlorosulfite calix[6]arene ion and chloride ion undergoes a chlorination to form *p-t*-butylcalix[6]arene acyl chloride.

3.1.2. Amidation reaction.

In order to create the *p-t*-butylcalix[6]arene ethylesteramide or the BEAC6ND4 ionophore, the second step involves the amidation reaction of the *p-t*-butylcalix[6]arene acyl chloride with ethyl 2-aminoacetate in dry tetrahydrofuran (Figure 6).

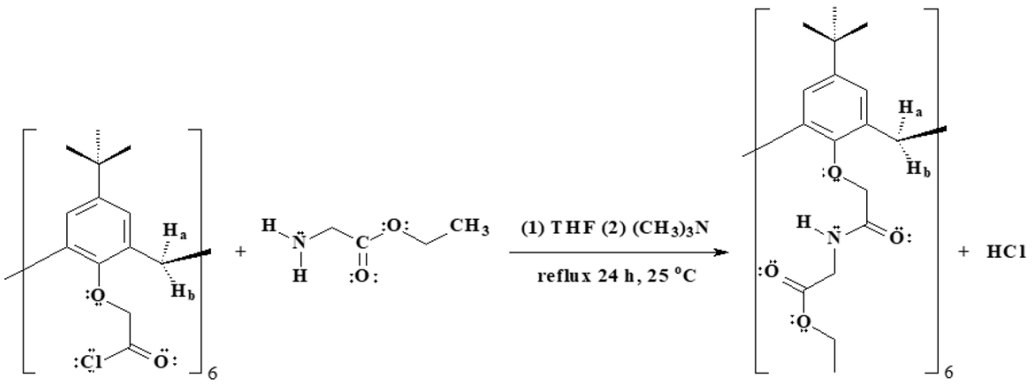

Figure 6. The BEAC6ND4 ionophore is created via the amidation reaction of *p-t*-butylcalix[6]arene acyl chloride with ethyl 2-aminoacetate.

A white solid with a randemen of 65.30%, a melting point of 345-347°C, and TLC (SiO_2, CH_3OH: CH_2Cl_2 = 1: 1 v/v, R_f = 0.79) was the synthesis result of the BEAC6ND4 ionophore. The synthesis product's R_f value (0.79) is greater than the reactant's R_f value (0.69)

(Figure 7). When the BEAC6ND4 ionophore has a lower polarity than the reactant, this is in line with expectations.

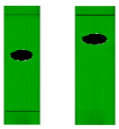

(a) **(b)**

Figure 7. Results of the TLC (SiO_2, CH_3OH: CH_2Cl_2 = 1 : 1 v/v) test: **(a)** Acyl chloride of *p-t*-butylcalix[6]arene (R_f = 0.69); **(b)** Ethylesteramide of *p-t*-butylcalix[6]arene (R_f = 0.79).

Figure 6 shows the synthesis of the BEAC6ND4 ionophore from p-t-butylcalix[6]arene acyl chloride. The following reaction scheme shows the reaction mechanism of the synthesis of the compound BEAC6ND4 ionophore from p-t-butylcalix[6]arene acyl chloride. The nucleophilic addition of amine to the carbonyl group is the first step of the amine acylation (amidation) reaction. Ethyl-2-aminoacetate (amine 1°) functions as a nucleophile to add to the carbonyl group of the acyl chloride compound to form a tetrahedral intermediate (Figure 8).

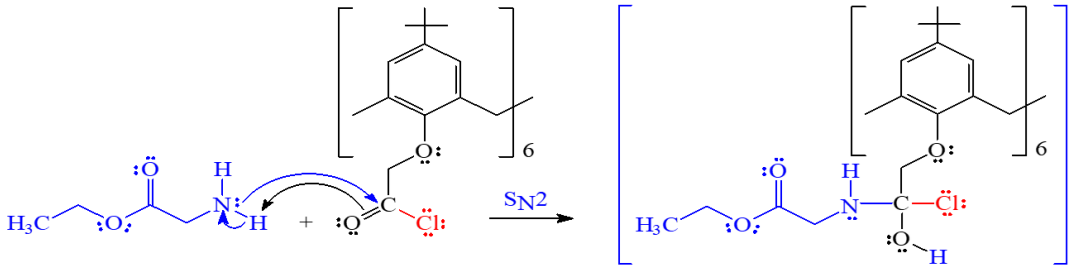

Figure 8. The reaction of ethyl-2-aminoacetate and acyl chloride calix[6]arene to form a tetrahedral intermediate.

In the final stage of the amidation reaction, the tetrahedral intermediate (Brønsted acid) dissociates to form an amide compound (BEAC6ND4 ionophore) through an acid-base reaction with ethyl-2-aminoacetate (amine 1°) (Brønsted base) (Figure 9).

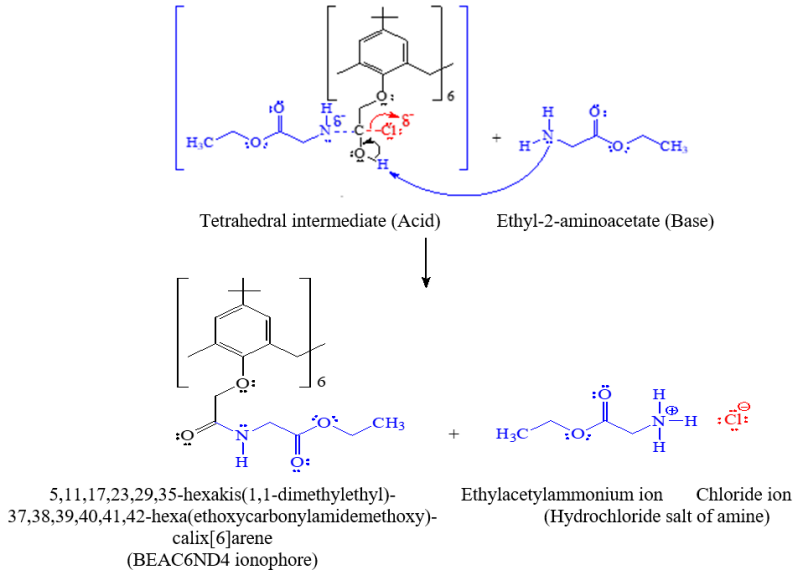

Figure 9. The reaction of the tetrahedral intermediate and ethyl-2-aminoacetate to form a BEAC6ND4 ionophore.

3.2. Characterization of the BEAC6ND4 Ionophore using FTIR.

Figure 10 and Table 1 compare and explain the FTIR spectra of the BEAC6ND4 ionophore (product) and *p-t*-butylcalix[6]arene carboxylic acid (raw material). Strong absorption bands at 3429.43 cm^{-1} and 1757.15 cm^{-1}, which are produced from the OH and C=O stretches of carboxylic acids, are visible in the FTIR spectra of the raw material, *p-t*-butylcalix[6]arene carboxylic acid. The BEAC6ND4 ionophore's FTIR spectrum does not show these two extremely strong absorption bands. The BEAC6ND4 ionophore's FTIR spectrum, on the other hand, revealed five very strong absorption bands at 1749.44 cm^{-1} (C=O stretch), 1114.86 cm^{-1} (C-O-C stretch in dialkyl ethers), 3446.79 and 3147.83 cm^{-1} (N-H stretch of secondary amides), 1645.28 cm^{-1} (C=O stretch of secondary amides [amide I band]), and 1483.26 cm^{-1} (C-N stretch of secondary amides [amide II band]). These five extremely strong absorption bands were absent from the raw material's FTIR spectrum, indicating that the synthesis reaction converted the raw material's OH and C=O groups of carboxylic acids into C=O esters, C-O-C ether, C=O amide, and C-N amide groups in the BEAC6ND4 ionophore.

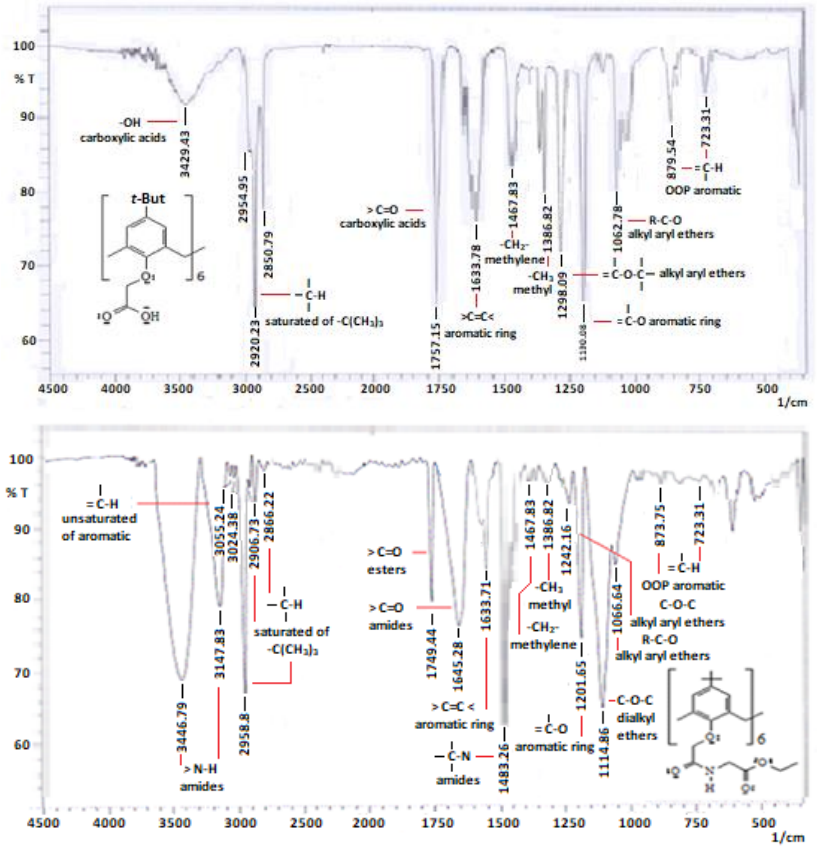

Figure 10. The FTIR spectra of the *p-t*-butylcalix[6]arene carboxylic acid (raw material) (top) and BEAC6ND4 ionophore (product) (bottom).

Table 1. Analysis of the FTIR spectra of the BEAC6ND4 ionophore (product) and *p-t*-butylcalix[6]arene carboxylic acid (raw material) [21-23].

No	Frequency (cm^{-1}) and intensities		Frequency ranges (cm^{-1}) and Intensities*	Group or Class	Remarks
	Raw material	BEAC6ND4 ionophore			
1	3429.43 (s)	-	3400-2400 (s)	Carboxylic Acids	OH stretch
2	1757.15 (vs)	-	1730-1700 (vs)	RCOOH	C=O stretch
3	-	1749.44 (s)	1765-1720 (vs)	Esters RCOOR’	C=O stretch
4	-	1114.86 (vs)	1140-1110 (vs)	Ethers ROR’	C-O-C stretch in dialkyl ethers
5	1298.09 (s)	1242.16 (m)	1280-1220 (s)		C-O-C stretch in alkyl aryl ethers

No	Frequency (cm^{-1}) and intensities		Frequency ranges (cm^{-1}) and Intensities*	Group or Class	Remarks
	Raw material	BEAC6ND4 ionophore			
6	1062.78 (m)	1066.64 (m)	1075-1020 (s)		R-C-O stretch in alkyl aryl ethers
7	-	3055.24 (w)	3159-3000 (m)	Aromatic ArH 	
8	-	3024.38 (w)			C-H stretch of unsaturated
9	1633.78 (m)	1633.71 (m)	1630-1430 (v)		C=C stretch of aromatic ring
10	1190.08 (vs)	1201.65 (vs)	1300-1000 (s)		C-O stretch of aromatic ring
11	879.54 (m)	873.75 (m)	900-650 (s)		Out-of-plane C-H deformation 1,4-disubstituted *para*
12	723.31 (m)	723.31 (m)			

No	Frequency (cm^{-1}) and intensities		Frequency ranges (cm^{-1}) and Intensities*	Group or Class	Remarks
	Raw material	BEAC6ND4 ionophore			
13	-	3446.79 (vs)	3460-3400 (m)	Amides CONHR	N-H stretch of secondary amides
14	-	3147.83 (s)	3200-3070 (m)		
15	-	1645.28 (s)	1680-1640 (vs)		C=O stretch of secondary amides (amide I band)
16	-	1483.26 (vs)	1550-1460 (s)		C-N stretch of secondary amides (amide II band)
17	2954.95 (w)	2958.8 (vs)	2970-2850 (s)	Aliphatic RH	C-H saturated stretching from $(CH_3)_3C$-
18	2920.23 (vs)	2906.73 (w)			
19	2850.79 (s)	2866.22 (w)			
20	1386.82 (m)	1394.53 (m)	1450-1375 (s)	*t*-Butyl $(CH_3)_3C$-	C-H stretch from CH_3-
21	1467.83 (m)	1458.18 (m)	1485-1450 (m)	Methylene $-CH_2$-	C-H stretch from $–CH_2$-

◦Notes: vs = *very strong*; v = *variable*; s = *strong*; m = *medium*; w = *weak*.

3.3. Characterization of the BEAC6ND4 Ionophore using NMR.

3.3.1. Characterization with ^{1}H-NMR.

The ^{1}H-NMR spectrum data of the synthesis result further support the success of this synthesis step. Figure 11 and Table 2 compare and interpret the NMR (^{1}H, ^{13}C) spectra of the BEAC6ND4 ionophore (product) and *p-t*-butylcalix[6]arene carboxylic acid (raw material).

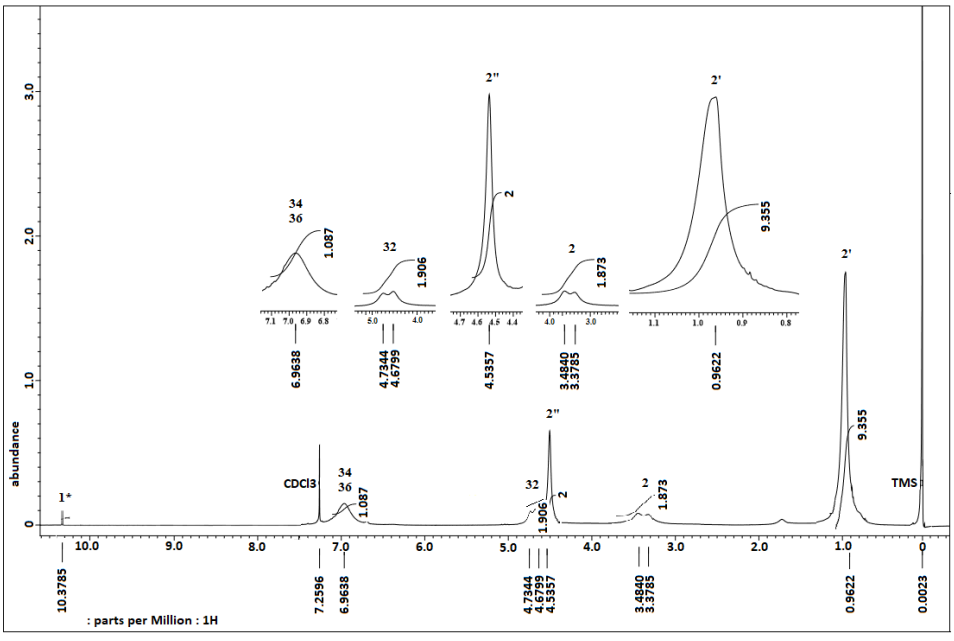

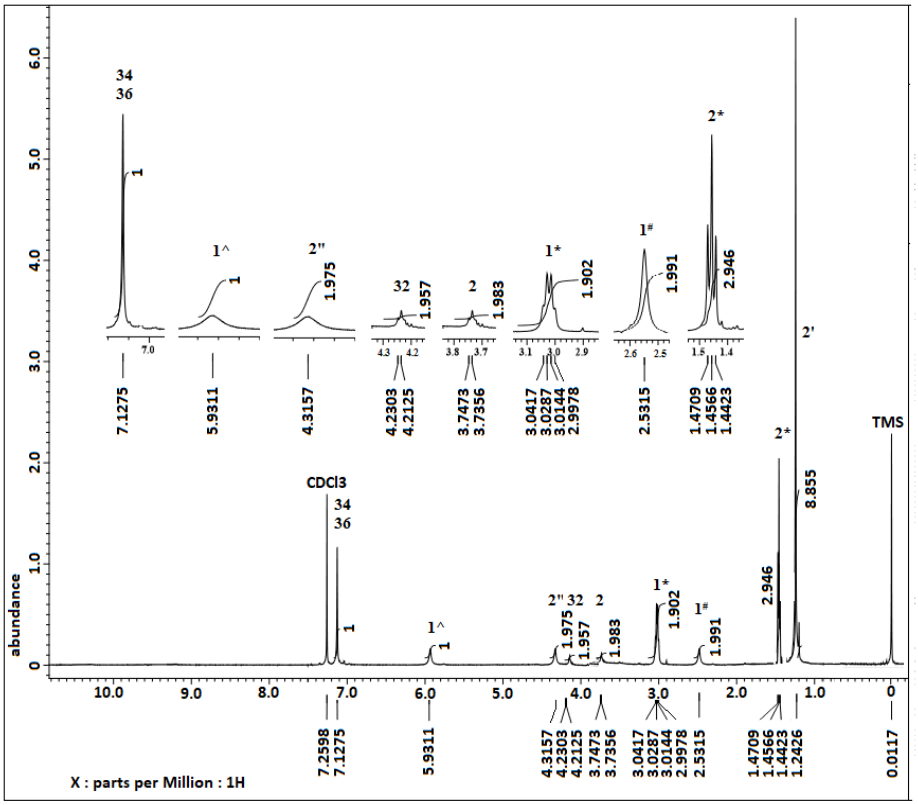

Figure 11. The ^{1}H-NMR spectrum of the *p-t*-butylcalix[6]arene carboxylic acid (raw material) (top) and BEAC6ND4 ionophore (product) (bottom).

Table 2. Analysis of the NMR (^{1}H, ^{13}C) spectra of the BEAC6ND4 ionophore (product) and *p-t*-butylcalix[6]arene carboxylic acid (raw material).

C position	δ_C (ppm)		Groups	H position	δ_H (ppm)		Groups
	Raw material	BEAC6ND4 ionophore			Raw material	BEAC6ND4 ionophore	
1, 33	132.9196	127.0885	**C**-*o* aryl	-	-	-	-
34, 36	126.4717	126.3255	**C**-*m* aryl	34, 36	6,9638 (1**H**, *s*)	7.1275 (1**H,** *s*)	Ar**H**
35	146.6262	144.4292	**C**-*p* aryl	-	-	-	-
37	153.2751	146.7315	**C**-O aryl	-	-	-	-
1'	34.0739	34.1757	**C**(CH_3)$_3$	-	-	-	-
2'	31.3746	31.6576	C(**C**H_3)$_3$	2'	0,9622 (9**H**, *s*)	1.2426 (9**H**, *s*)	C(C**H**$_3$)$_3$
2, 32	31.6131	33.1742	Ar**C**H_2Ar	$2_{a, b}$ exo	3,4313 (2**H,** *d*, *J* = 12.9 Hz)	3.7415 (2**H,** *d*, *J* = 12.9 Hz)	ArC**H**$_2$Ar
				32 endo	4,7071 (2**H,** *d*, *J* = 12,9 Hz)	4.2214 (2**H,** *d*, *J* = 12.9 Hz)	ArC**H**$_2$Ar
1"	169.6231	-	**C**=O carboxylic acids	1"	10,3785 (1**H**, *s*)	-	CO_2**H**
	-	172.2135	**C**=O amides		-	-	-
2"	70.8060	73.4327	ArO**C**H_2-	2"	4,5357 (2**H**, *s*)	4.3157 (2**H,** *s*)	C**H**$_2$O
1^	-	-	-	1^	-	5.9311 (1**H,** *s*)	N**H**
$1^{\#}$	-	42.3405	**C**H_2 amides	$1^{\#}$	-	2.5315 (2**H,** *s*)	C**H**$_2$NH
$2^{\#}$	-	170.3562	**C**=O esters	-	-	-	-
1*	-	62.6373	**C**H_2 esters	1*	-	3.0216 (2**H,** *q*, *J* = 6.7 Hz)	OC**H**$_2$CH$_3$
2*	-	11.3696	**C**H_3 esters	2*	-	1.4566 (3**H,** *t*, *J* = 6.7 Hz)	OCH$_2$C**H**$_3$

• Notes: o = ortho; m = meta; p = para; s = singlet; d = doublet; m = multiplet; J = coupling constant.

A signal from carboxylic acid protons (O**H**-1*) is detected at δ_H 10,3785 ppm (1**H**, s) in the ^{1}H-NMR spectrum of the raw material, *p*-*t*-butylcalix[6]arene carboxylic acid. The BEAC6ND4 ionophore's ^{1}H-NMR spectrum no longer contains this signal. However, the BEAC6ND4 ionophore's ^{1}H-NMR spectrum reveals a number of signals that are absent from the raw material's ^{1}H-NMR spectrum. These signals include the amide (N**H**-1^) proton signal at δ_H 5.9311 ppm (1**H**, s), the methylene amide (C**H**$_2$NH-1#) proton signal at δ_H 2.5315 ppm (2**H**, s), the methylene ethoxy (OC**H**$_2$CH$_3$-1*) proton signal at δ_H 3.0216 ppm (2**H**, q, *J* = 6.7 Hz), and the methyl ethoxy (OCH$_2$C**H**$_3$-2*) proton signal at δ_H 1.4566 ppm (3**H**, t, *J* = 6.7 Hz). This indicates that in the BEAC6ND4 ionophore, the raw material's OH group has changed into ethylesteramide. Moreover, the BEAC6ND4 ionophore displays proton signals identical to those of the raw material. These signals include the aryl (Ar**H**-34/36) proton signal at δ_H 7.1275 ppm (1**H**, s), the methylene methoxy (C**H**$_2$O-2") proton signal at δ_H 4.3157 ppm (2**H**, s), the methylene bridge proton signal, which is divided into two signals: the exo methylene (ArC**H**$_2$Ar-2$_{a,b}$) bridge proton signal at δ_H 3.7415 ppm (2**H**, d, *J* = 12.9 Hz) and the endo methylene (ArC**H**$_2$Ar-32) bridge proton signal at δ_H 4.2214 ppm (2**H**, d, *J* = 12.9 Hz), and the highest-intensity singlet proton signal at δ_H 1.2426 ppm (9**H**, s) that comes from tert-butyl (C(C**H**$_3$)$_3$-2'). As a result, the signals in the ^{1}H-NMR spectra of the produced product that fall between δ_H 0 and 7.0 ppm correspond to the proton character of the BEAC6ND4 ionophore (Figure 12).

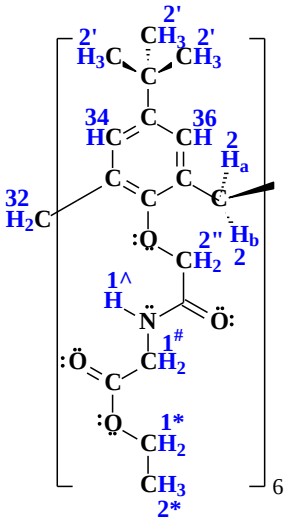

Figure 12. The ionophore BEAC6ND4's proton character.

3.3.2. Characterization with ^{13}C-NMR.

Figure 13 and Table 2 compare and interpret the ^{13}C-NMR spectra of the BEAC6ND4 ionophore (product) and *p*-*t*-butylcalix[6]arene carboxylic acid (raw material). The results of the FTIR and ^{1}H-NMR spectrum analysis above were also supported by the ^{13}C-NMR spectrometer's study of the synthesis product. A signal from carbon **C**-1" that binds to the **C**=O amide group was detected at δ_C 172.2135 ppm in the ^{13}C-NMR spectra of the BEAC6ND4 ionophore. In contrast, the raw material's ^{13}C-NMR spectra show the **C**-1" carbon signal at δ_C 169,6231 ppm as a **C**=O carboxylic acid group. This indicates that the **C**=O amide group on the BEAC6ND4 ionophore has replaced the **C**=O carboxylic acid group on the raw material. Additionally, a number of signals that are absent from the raw material's ^{13}C-NMR spectrum are present in the ^{13}C-NMR spectrum of the BEAC6ND4 ionophore. These signals include the carbonyl ester (**C**=O ester) (**C**-2$^{\#}$) signal at δ_C 170.3562 ppm, the methylene amide (**C**H$_2$NH-

1[#]) (**C**-1[#]) signal at δ_C 42.3405 ppm, the methylene ethoxy (O**C**H$_2$CH$_3$-1*) (**C**-1*) signal at δ_C 62.6373 ppm, and the methyl ethoxy (OCH$_2$**C**H$_3$-2*) (C-2*) signal at δ_C 11.3696 ppm. This indicates that the BEAC6ND4 ionophore's carbon framework has grown by four C atoms.

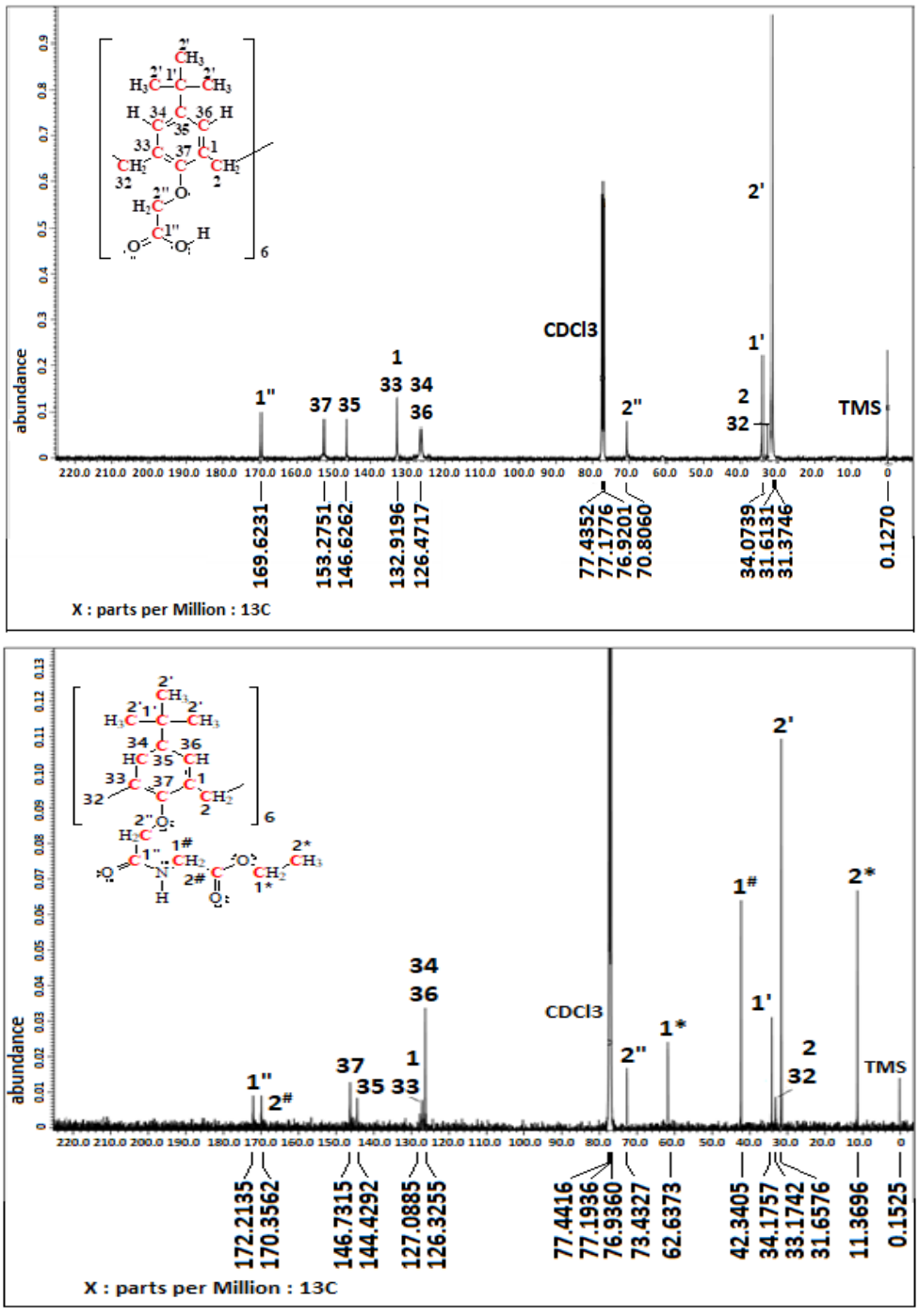

Figure 13. The [13]C-NMR spectrum of the *p*-*t*-butylcalix[6]arene carboxylic acid (raw material) (top) and BEAC6ND4 ionophore (product) (bottom).

The carbon signals from the raw material are identical to the other carbon signals that show up in the [13]C-NMR spectra of the BEAC6ND4 ionophore. These signals correspond to aryl carbon (**C**-aryl) atoms that are dispersed among four δ_C values. First, the **C**-37 (**C**-aryl) atomic signal, which binds oxygen directly to the OCH$_2$CONHR group, is the greatest *downfield* signal that can be seen at δ_C 146.7315 ppm. Second, the aryl **C**-35 atomic signal at *para* (**C**-*para* aryl) that attaches to the *t*-butyl group is the one that shows up at δ_C 144.4292 ppm. Third, the aryl **C**-1/**C**-33 atomic signal at the *ortho* (**C**-*ortho* aryl) position is the one that can be seen at δ_C 127.0885 ppm. Fourth, the aryl **C**-34/**C**-36 atomic signal at the *meta* (**C**-*meta*

aryl) position is the one that may be seen at δ_C 126.3255 ppm. Moreover, alkyl groups are the source of the signals from carbon atoms that appear farther *upfield*. The **C**-2" atomic signal from the methylene aryl ether carbon (ArO**C**H_2-) is the one that is detected at δ_C 73.4327 ppm. At δ_C 34.1757 ppm, the **C**-1' atomic signal from the *t*-butyl *quarterner* carbon [-**C**$(CH_3)_3$] is visible. The (**C**-2/**C**-32) atomic signal from the methylene bridge carbon (Ar**C**H_2Ar) is the one that is detected at δ_C 33.1742 ppm. At δ_C 31.6576 ppm, the **C**-2' atomic signal from *t*-butyl methyl carbon [-C(**C**$H_3)_3$] is visible. As a result, the signals that show up in the ^{13}C-NMR spectra of the synthesis product between δ_C 0 and 180.0 ppm correspond to the carbon framework of the BEAC6ND4 ionophore or *p-t*-butylcalix[6]arene ethyl ester amide (Figure 14).

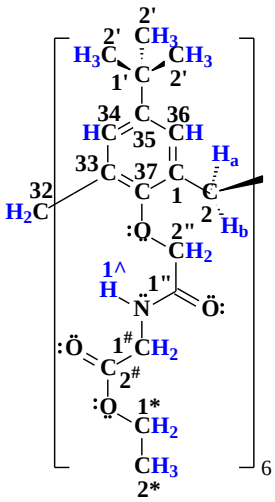

Figure 14. The BEAC6ND4 ionophore's carbon structure.

3.4. The BEAC4ND4 ionophore's conformational shape.

The BEAC6ND4 ionophore's conformational form is readily discernible from its ^{1}H and ^{13}C-NMR spectra, mostly thanks to the patterns for the bridging methylene groups. The conformations of calix[6]arenes are *cone* if the methylene proton's chemical shift is near (4.2 ± 1 ppm) and (3.4 ± 1 ppm) [24-36].

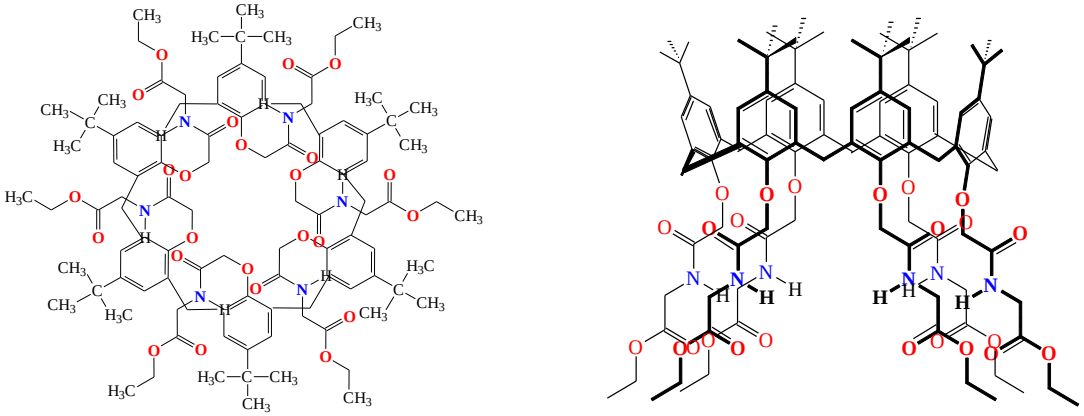

Figure 15. The BEAC6ND4 ionophore's *cone* conformation.

The methylene bridge proton (ArC**H**$_2$Ar) absorption band is visible as two *doublets* on δ_H 4.2214 ppm and δ_H 3.7415 ppm in the ^{1}H-NMR spectrum of the BEAC6ND4 ionophore (Table 2). This absorption band's pattern suggests that the BEAC6ND4 ionophore has a *cone*-like shape (Figure 15). Two nearby aryl groups are in a *syn* orientation to one

another if the methylene carbon's chemical shift is close to 31 ppm [18-22]. The methylene bridge group (Ar**C**H_2Ar) exhibits a carbon absorption band at δ_C 33.1742 ppm (~ 31 ppm) in the ^{13}C-NMR spectrum of the BEAC6ND4 ionophore (Table 2). This indicates that two neighboring aryl groups are oriented in a *syn* (a plot) relationship with one another (Figure 15). The 3D structure of the *cone* conformation of the BEAC6ND4 ionophore is shown in Figure 16.

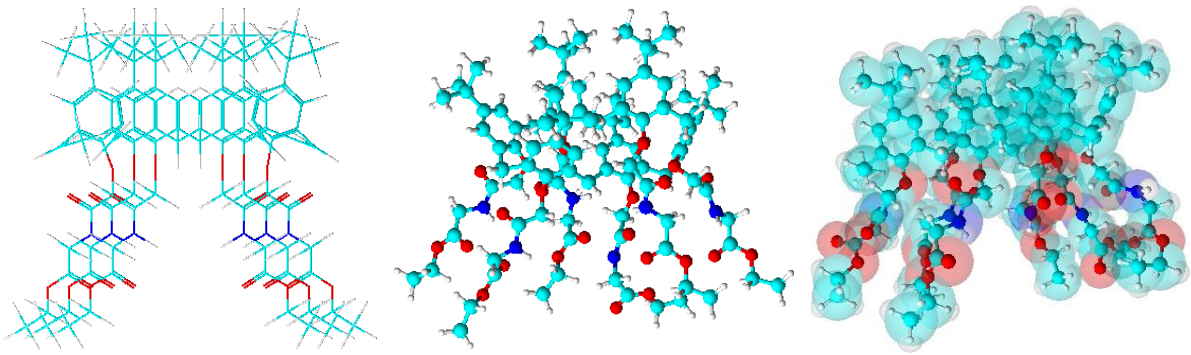

(a) **(b)**

Figure 16. The **(a)** 3D viewer of sticks; **(b)** 3D optimization of sticks and balls of the BEAC6ND4 ionophore's *cone* shape.

3.5. Interpretation of bond length, bond angle, and torsion angle data from the 3D viewer and 3D optimization structures of the BEAC4ND4 ionophore.

Table 3 shows the results of the calculation of bond length, bond angle, and torsion angle from the 3D viewer and 3D optimization structures of the BEAC4ND4 ionophore.

According to Table 3, before the structure of the BEAC6ND4 ionophore was optimized, all C-C bonds in the benzene ring had the same bond length (1.292 Å). However, after the structure of the BEAC6ND4 ionophore was optimized, the C-C bond length of the benzene ring became 1.411 Å, which is exactly midway between the length of the sp^3-sp^3 single bond (1.46 Å) and the length of the sp^2-sp^2 double bond (1.34 Å). These data prove that benzene does not have alternating single and double bonds. This indicates that benzene is not a cyclohexatriene or a pair of isomers that equilibrate rapidly. After the structure of the BEAC6ND4 ionophore was optimized, the C-C-C bond angle of benzene (120°) remained unchanged. These data indicate that the molecular geometry of benzene is planar, and its carbon skeleton is regular hexagonal. After the structure of the BEAC6ND4 ionophore was optimized, the torsion angle of benzene (0°) changed to C-C-C-C (359.554°≈ 360°), which indicates that benzene in the BEAC6ND4 ionophore structure underwent a rotation of 360°.

According to Table 3, all C-C and C-H bonds in the *t*-butyl group [$C(CH_3)_3$] have the same bond length (1.292 Å) before the structure of the BEAC6ND4 ionophore was optimized. After the structure of the BEAC6ND4 ionophore was optimized, the lengths of C-C and C-H bonds in the *t*-butyl group [$C(CH_3)_3$] changed to (1.58 Å) and (1.135 Å), respectively. These data indicate that the lengths of C-C and C-H bonds in the *t*-butyl group [$C(CH_3)_3$] are similar to the lengths of C-C (1.58 Å ≈ 1.53 Å) and C-H (1.135 Å ≈ 1.11 Å) bonds in alkanes. After the structure of the BEAC6ND4 ionophore was optimized, the C-C-C bond angle (120°) of the *t*-butyl group [$C(CH_3)_3$] remained unchanged. The molecular geometry of the *t*-butyl group [$C(CH_3)_3$] is trigonal planar, as shown by these data. After the structure of the BEAC6ND4 ionophore was optimized, the torsion angle of the *t*-butyl group [$C(CH_3)_3$] changed to C-C-C-C (328.401° ≈ 330°). The data showed that the *t*-butyl group [$C(CH_3)_3$] in the BEAC6ND4 ionophore structure underwent a rotation of 330° after optimization.

Table 3. Data of bond length, bond angle, and torsion angle before and after the BEAC6ND4 ionophore structure was optimized.

C Position	H Position	Groups	Bonds	Bond Length (Å)		Bonds	Bond Angle (°)		Bonds	Torsion Angle (°)	
				3D V	3D O		3D V	3D O		3D V	3D O
1, 33	-	**C**-*o* aryl	C_1-C_2	1.292	1.571	C_{37}-C_1-C_2	240.004	234.79	C_1-C_{36}-C_{35}-C_{34}	0	2.716
			C_1-C_{36}	1.292	1.419	C_{36}-C_1-C_2	120.003	115.218	C_1-C_{36}-C_{35}- $C_{1'}$	180	183.772
			C_1-C_{37}	1.292	1.437	C_{37}-C_1-C_{36}	120.001	119.571	C_1-C_{37}-C_{33}-C_{32}	180	179.489
									C_1-C_{37}-C_{33}-C_{34}	0	1.549
									C_1-C_{37}-O- $C_{2''}$	180	334.26
			C_{33}-C_{32}	1.292	1.567	C_{37}-C_{33}-C_{32}	120.005	122.19	C_{33}-C_{34}-C_{35}-C_{36}	0	358.419
			C_{33}-C_{34}	1.292	1.417	C_{34}-C_{33}-C_{32}	240.004	242.348	C_{33}-C_{34}-C_{35}- $C_{1'}$	180	177.396
			C_{33}-C_{37}	1.292	1.427	C_{37}-C_{33}-C_{34}	340.004	239.872	C_{33}-C_{37}-C_1-C_2	180	179.078
									C_{33}-C_{37}-C_1-C_{36}	0	359.554
									C_{33}-C_{37}-O- $C_{2''}$	180	154.578
34, 36	34, 36	**C**-*m* aryl Ar**H**	C_{34}-H	1.292	1.132	C_{33}-C_{34}-H	120.001	119.707	C_{34}-C_{35}-C_{36}- H	180	182.355
									C_{34}-C_{35}-C_{36}- C_1	0	2.716
			C_{34}-C_{35}	1.292	1.413	C_{35}-C_{34}-H	240	240.856	C_{34}-C_{35}-$C_{1'}$- $C_{2'}$	180	171.615
			C_{34}-C_{33}	1.292	1.417	C_{33}-C_{34}-C_{35}	240.001	238.851	C_{34}-C_{33}-C_{32}-H	180	201.132
									C_{34}-C_{33}-C_{37}- C_1	0	1.549
									C_{34}-C_{33}-C_{37}- O	180	181.248
			C_{36}-H	1.292	1.134	C_1-C_{36}-H	240.019	240.89	C_{36}-C_{35}-C_{34}- H	180	178.726
									C_{36}-C_{35}-C_{34}- C_{33}	0	358.419
			C_{36}-C_{35}	1.292	1.411	C_{35}-C_{36}-H	120.015	119.485	C_{36}-C_{35}-$C_{1'}$- $C_{2'}$	180	230.51
			C_{36}-C_1	1.292	1.419	C_1-C_{36}-C_{35}	120.004	121.405	C_{36}-C_1-C_2-H	180	177.005
									C_{36}-C_1-C_{37}- C_{33}	0	359.553
									C_{36}-C_1-C_{37}- O	180	179.876
35	-	**C**-*p* aryl	C_{35}-C_{34}	1.292	1.413	C_{34}-C_{35}-C_{36}	240.006	241.18	C_{35}-C_{34}-C_{33}- C_{32}	0	181.427
			C_{35}-C_{36}	1.292	1.411	C_{34}-C_{35}-$C_{1'}$	120.004	119.056	C_{35}-C_{34}-C_{33}- C_{37}	0	359.458
									C_{35}-$C_{1'}$-$C_{2'}$- H	180	159.512
			C_{35}-$C_{1'}$	1.292	1.571	C_{36}-C_{35}-$C_{1'}$	239.998	237.883	C_{35}-C_{36}-C_1- C_2	180	178.719
									C_{35}-C_{36}-C_1- C_{37}	0	358.289
37	-	**C**-O aryl	C_{37}-O	1.292	1.406	C_{33}-C_{37}-O	240	242.719	C_{37}-O-$C_{1''}$-$C_{2''}$	180	103.338
									C_{37}-O-$C_{1''}$-H	180	341.158
			C_{37}- C_1	1.292	1.437	C_1-C_{37}-O	119.998	123.847	C_{37}- C_1-C_2- H	0	357.462
									C_{37}-C_1-C_{36}- H	180	178.649
									C_{37}-C_1-C_{36}- C_{35}	0	358.289
			C_{37}- C_{33}	1.292	1.427	C_{33}-C_{37}- C_1	120.002	118.872	C_{37}- C_{33}-C_{32}- H	0	144.371
									C_{37}- C_{33}-C_{34}- H	180	179.15
									C_{37}- C_{33}-C_{34}- C_{35}	0	359.458
1’	**C**$(CH_3)_3$	*t*-butyl	$C_{1'}$-C_{35}	1.292	1.571	C_{35}-$C_{1'}$-$C_{2'}$	240.004	110.856	$C_{1'}$-C_{35}-C_{36}-H	0	358.662
									$C_{1'}$-C_{35}-C_{36}- C_1	180	183.772

C Position	H Position	Groups	Bonds	Bond Length (Å)		Bonds	Bond Angle (°)		Bonds	Torsion Angle (°)	
				3D V	3D O		3D V	3D O		3D V	3D O
			$C_{1'}$-$C_{2'}$	1.292	1.58	$C_{2'}$-$C_{1'}$-$C_{2'}$	120.005	107.678	$C_{1'}$-C_{35}- C_{34}-H	0	357.703
									$C_{1'}$-C_{35}- C_{34}- C_{33}	180	183.829
2'	2'	C(CH_3)$_3$ *t*-butyl	$C_{2'}$-H	1.292	1.135	$C_{1'}$-$C_{2'}$-H	90/180	249.526	$C_{2'}$-$C_{1'}$- C_{35}-C_{36}	0/180	151.72
			$C_{2'}$-$C_{1'}$-	1.292	1.58				$C_{2'}$-$C_{1'}$- C_{35}-C_{34}	0/180	328.401
2	$2_{a, b}$ exo	ArCH_2Ar bridges	C_2-H	1.292	1.133	C_1-C_2-H	60.003	106.389	C_2-C_1-C_{36}-H	0	359.078
							240.003	249.09	C_2-C_1-C_{36}-C_{35}	180	178.719
			C_2-C_1	1.292	1.571	H-C_2-H	180	106.973	C_2-C_1-C_{37}- O	0	359.4
									C_2-C_1-C_{37}- C_{33}	180	179.078
32	32 endo	ArCH_2Ar bridges	C_{32}-H	1.292	1.138	C_{33}- C_{32}-H	120.002	109.567	C_{32}-C_{33}-C_{34}-H	0	1.118
							300.002	248.94	C_{32}-C_{33}-C_{34}-C_{35}	180	181.427
			C_{32}-C_{33}	1.292	1.567	H-C_{32}-H	180	109.604	C_{32}-C_{33}-C_{37}-O	0	359.187
									C_{32}-C_{33}-C_{37}- C_1	180	179.489
1"	-	**C**=O amides	$C_{1"}$=O	1.292	1.235	$C_{2"}$-$C_{1"}$=O	239.99	239.558	$C_{1"}$-$C_{2"}$-O-C_{37}	180	291.262
			$C_{1"}$ - N	1.268	1.532	$C_{2"}$-$C_{1"}$-N	119.999	118.685	$C_{1"}$-N- $C_{1\#}$-H	0	326.218
										180	206.872
			$C_{1"}$ - $C_{2"}$	1.268	1.409	N-$C_{1"}$=O	119.992	120.792	$C_{1"}$-N- $C_{1\#}$-$C_{2\#}$	180	85.61
2"	2"	ArO**C**H_2 CH_2O ethers	C_{37}-O	1.292	1.406	C_{37}-O-$C_{2"}$	180	202.461	C_{37}-O- $C_{2"}$-$C_{1"}$	180	291.262
									C_{37}-O- $C_{2"}$-H	180	170.989
			$C_{2"}$-H	1.292	1.134	$C_{1"}$-$C_{2"}$-H	59.998	107.137	$C_{2"}$-$C_{1"}$-N-$H_{1\wedge}$	0	4.282
							239.998	254.515			
			$C_{2"}$- $C_{1"}$	1.268	1.532	$C_{1"}$-$C_{2"}$-O	119.996	115.519	$C_{2"}$-$C_{1"}$-N- $C_{1\#}$	180	212.188
			$C_{2"}$-O	1.292	1.484	H-$C_{2"}$-H	180	251.398	$C_{2"}$-O-C_{37}-C_{33}	180	105.078
									$C_{2"}$-O-C_{37}-C_1	180	284.729
-	1^	N**H** amides	N-$H_{1\wedge}$	1.292	1.027	$C_{1"}$-N-$H_{1\wedge}$	119.998	122.916	N-$C_{1"}$-$C_{2"}$-H	0	137.148
										180	21.565
			N- $C_{1"}$	1.268	1.409				N-$C_{1"}$-$C_{2"}$-O	180	258.152
			N- $C_{1\#}$	1.268	1.502	$C_{1"}$-N-$C_{1\#}$	240.003	236.119	N-$C_{1\#}$-$C_{2\#}$=O	0	242.197
									N-$C_{1\#}$-$C_{2\#}$-O	180	62.041
$1^{\#}$	$1^{\#}$	**C**H_2 CH_2NH amides	$C_{1\#}$-H	1.292	1.136	N-$C_{1\#}$-H	59.999	251.621	$C_{1\#}$-N-$C_{1"}$=O	0	28.913
							239.999	109.183			
						H-$C_{1\#}$-H	179.999	250.388			
			$C_{1\#}$-N	1.268	1.502	N-$C_{1\#}$-$C_{2\#}$	119.995	112.428	$C_{1\#}$-N-$C_{1"}$-$C_{2"}$	180	212.188
							300.002	108.073			
			$C_{1\#}$-$C_{2\#}$	1.268	1.558	$C_{2\#}$-$C_{1\#}$-H	120.004	109.13	$C_{1\#}$-$C_{2\#}$-O-C_{1*}	180	350.825
$2^{\#}$	-	**C**=O esters	$C_{2\#}$=O	1.292	1.235	$C_{1\#}$-$C_{2\#}$=O	120.001	240.856	$C_{2\#}$-$C_{1\#}$-N-$H_{1\wedge}$	0	290.046
			$C_{2\#}$-O	1.268	1.397	$C_{1\#}$-$C_{2\#}$-O	239.997	122.198	$C_{2\#}$-$C_{1\#}$-N-$C_{1"}$	180	85.61
			$C_{2\#}$-$C_{1\#}$	1.268	1.558	O-$C_{2\#}$=O	240.004	118.658	$C_{2\#}$-O-C_{1*}-H	0	295.586
										180	55.715
									$C_{2\#}$-O-C_{1*}-C_{2*}	180	175,829

C Position	H Position	Groups	Bonds	Bond Length (Å)		Bonds	Bond Angle (°)		Bonds	Torsion Angle (°)	
				3D V	3D O		3D V	3D O		3D V	3D O
1*	1*	**C**H_2 OCH_2CH_3 esters	C_{1*}-H	1.292	1.133	O-C_{1*}-H	120.001	110	C_{1*}-O-$C_{2\#}$=O	0	170.669
							300.002	108.845			
						H-C_{1*}-H	180	250			
			C_{1*}-O	1.268	1.449	O-C_{1*}-C_{2*}	240.002	248.11	C_{1*}-O-$C_{2\#}$-$C_{1\#}$	180	350.825
			C_{1*}-C_{2*}	1.268	1.554	H-C_{1*}-C_{2*}	120.001	108.173			
							300.001	251.327			
2*	2*	**C**H_3 OCH_2CH_3 esters	C_{2*}-H	1.292	1.134	C_{1*}-C_{2*}-H	90	249.895	C_{2*}-C_{1*}-O-$C_{2\#}$	180	179.015
							180	109.008			
							270	67.387			
			C_{2*}-C_{1*}	1.268	1.554	H-C_{2*}-H	90	250.707			
							180	103.603			
							270	274.351			

Notes: 3D V = 3D Viewer; 3D O = 3D Optimization.

According to Table 3, all C-C and C-H bonds in the methylene bridge group ($ArCH_2Ar$) have the same bond length (1.292 Å) before the BEAC6ND4 ionophore structure was optimized. However, after optimization, the C-C and C-H bond lengths in the methylene bridge group ($ArCH_2Ar$) changed to 1.571 Å and 1.133 Å, respectively. These data indicate that the C-C and C-H bond lengths in the methylene bridge group ($ArCH_2Ar$) in the BEAC6ND4 ionophore structure after optimization are similar to the C-C (1.571 Å ≈ 1.53 Å) and C-H (1.133 Å ≈ 1.11 Å) bond lengths in alkanes. After the structure of the BEAC6ND4 ionophore was optimized, the bond angles of C-C-H (120.002°) and H-C-H (180°) in the methylene bridge group ($ArCH_2Ar$) were changed to C-C-H (109.567° ≈ 109.5°) and H-C-H (109.604° ≈ 109.5°), respectively. The data showed that the molecular geometry of the methylene bridge group ($ArCH_2Ar$) was tetrahedral. After the structure of the BEAC6ND4 ionophore was optimized, the torsion angles of C-C-C-H (0°) and C-C-C-C (180°) were changed to C-C-C-H (359.078° ≈ 360°) and C-C-C-C (181.427° ≈ 180°), respectively. The data show that the $-CH_2-$ group on the methylene bridge ($ArCH_2Ar$) in the BEAC6ND4 ionophore structure underwent a rotation of 360° after optimization.

According to Table 3, before the structure optimization of the BEAC6ND4 ionophore, the C-C and C-N bond lengths in the amide group ($CH_2C{=}ONHCH_2$) were 1.268 Å, while the C=O, N-H, and C-H bond lengths were 1.292 Å. After structure optimization, the C-C and C-N bond lengths in the amide group changed to 1.558 Å and 1.409 Å, respectively. The C-N bond length of amide (1.409 Å) lies between the C-C bond distance in alkanes (1.53 Å) and the C-O bond distance in alcohols and ethers (1.43 Å). However, the bond lengths of C=O, N-H, and C-H change to (1.235 Å), (1.027 Å ≈ 1.01 Å), and (1.136 Å ≈ 1.11 Å), respectively. The C=O bond length in amides (1.235 Å) is shorter than the C-O bond length in alcohols and ethers (1.43 Å). Before optimization, the BEAC6ND4 ionophore structure has C-C=O, C-N-C, and N-C-H bond angles in the amide group($CH_2C{=}ONHCH_2$) of (240.003° ≈ 240°), while the C-C-N, N-C=O, C-N-H, N-C-C, and C-C-H bond angles in the amide group ($CH_2C{=}ONHCH_2$) are (119,999° ≈ 120°). After optimization, the C-C=O, C-N-C, and N-C-H bond angles do not change (239.558° ≈ 240°). Similarly, the bond angles of C-C-N, N-C=O, C-N-H, N-C-C, and C-C-H are also unchanged (120.792° ≈ 120°), but these data indicate that the C-N-H bond angle in amides (120°) is slightly larger than the C-N-H bond angle in amines (112°). To reduce the repulsion between electron pairs, the nitrogen atom of amines has a tetrahedral geometry based on sp^3 hybridization. In contrast, the lone pair of electrons in the amide nitrogen is in a *p* orbital, which allows *p* to overlap with the *p* orbital on the carbonyl carbon atom. As a result, the nitrogen atom of amides has a trigonal planar geometry and sp^2 hybridization. The ionophore structure of BEAC6ND4 before optimization has torsion angles of C-N-C-H, N-C-C-H, N-C-C=O, and C-N-C=O in the amide group ($CH_2C{=}ONHCH_2$) of (0°), while the torsion angles of C-C-O-C, C-N-C-C, and N-C-C-O are (180°). After optimization, the torsion angles of C-N-C-H, N-C-C-H, N-C-C=O, and C-N-C=O in the amide group ($CH_2C{=}ONHCH_2$) change to (326.218° ≈ 326°), while the torsion angles of C-C-O-C, C-N-C-C, and N-C-C=O are changed to (350.825° ≈ 351°). These data show that after optimization, the amide group ($CH_2C{=}ONHCH_2$) in the BEAC6ND4 ionophore structure has undergone rotations of 326° and 351°.

The C-H, C-C, and C-O bond lengths in the ether group ($ArOCH_2$) changed to (1.134 Å), (1.532 Å), and (1.406 Å) after the structure of the BEAC6ND4 ionophore was optimized, as shown in Table 3. Previously, all C-H and C-O bonds in the ether group ($ArOCH_2$) had the

same bond length (1.292 Å), while the C-C bond length was 1.268 Å. The C-O bond length (1.406 Å) in the ether group ($ArOCH_2$) in the BEAC6ND4 ionophore structure after optimization is similar to the C-O bond length of alcohol (1.42 Å) and shorter than the C-C bond length of alkane (1.53 Å), while the C-H and C-C bond lengths are the same as the C-H (1.134 Å ≈ 1.11 Å) and C-C (1.532 Å ≈ 1.53 Å) bond lengths in alkanes. Before optimization, the BEAC6ND4 ionophore structure had a C-O-C bond angle in the ether group ($ArOCH_2$) of 180°. However, after optimization, the C-O-C bond angle in the ether group ($ArOCH_2$) changed to (202.461° ≈ 202.5°). The data show that the Van der Waals force involving the aryl and alkyl groups makes the ether bond angle (202.5°) larger than that of phenol (109°) and water (105°). The ether oxygen affects the molecular conformation in the same way as the -CH_2- unit. The most stable ether conformation is the anti-staggered conformation. Before optimization, the BEAC6ND4 ionophore structure had a C-O-C-C torsion angle of the ether group ($ArOCH_2$) of 180°. However, after optimization, the C-O-C-C torsion angle of the ether group ($ArOCH_2$) changed to (291.262° ≈ 291°). These data indicate that the ether group ($ArOCH_2$) in the BEAC6ND4 ionophore structure underwent a rotation of 291°.

According to Table 3, the C-C and C-O bond lengths in the ester group ($CH_2C{=}OOCH_2CH_3$) were 1.268 Å before the BEAC6ND4 ionophore structure was optimized, while the C=O and C-H bond lengths were 1.292 Å. After optimization, the C-C and C-O bond lengths in the ester group ($CH_2C{=}OOCH_2CH_3$) increased to 1.559 Å and 1.449 Å, respectively. The C-C bond length in esters (1.554 Å) is comparable to the C-C bond length in alkanes (1.53 Å), and the C-O bond distance in esters (1.449 Å) is comparable to the C-O bond distance in alcohols and ethers (1.43 Å), while the C=O and C-H bond lengths change to (1.235 Å) and (1.133 Å ≈ 1.11 Å), respectively. The C=O bond distance in esters (1.235 Å) is shorter than the C-O bond distance in ethers and alcohols (1.43 Å), and the C-H bond distance in esters (1.133 Å) is almost the same as the C-H bond distance in alkanes (1.11 Å). Before optimization, the BEAC6ND4 ionophore structure has C-C=O, O-C=O, and C-C-O bond angles in the ester group ($CH_2C{=}OOCH_2CH_3$) of (120.001°), (240.004°), and (239.997°). After optimization, the bond angles of C-C=O, O-C=O, and C-C-O in the ester group changed to (240.856° ≈ 240°), (118.658° ≈ 120°), and (122.198° ≈ 120°), respectively. The molecular geometry of the ester is coplanar (120°) with respect to the carbonyl group (C=O), as indicated by these data. The C=O bond in the ester can be described by the sp^2 hybridization model of ethylene. According to this model, the C=O bond can be considered as one of the σ + π types. The σ component is generated by the overlap of the half-filled sp^2 hybrid orbitals of carbon and oxygen, and the π bond is generated by the side-by-side overlap of the half-filled 2*p* orbitals. The oxygen lone pair occupies the sp^2 hybrid orbital whose axes lie in the plane of the molecule. Before optimization, the structure of the BEAC6ND4 ionophore had a C-O-C=O torsion angle in the ester group (CH2C=$OOCH_2CH_3$) of (0°). The C-O-C=O torsion angle of the ester group in the BEAC6ND4 ionophore structure changes to (170.669° ≈ 171°), which indicates that the ester group undergoes a rotation of 171° after the structure is optimized.

4. Conclusions

The *p*-*t*-butylcalix[6]arene carboxylic acid has been effectively converted into the BEAC6ND4 ionophore. The chlorination and amidation reactions were the two stages of the synthesis procedure that produced the BEAC6ND4 ionophore. The *p*-*t*-butylcalix[6]arene acyl chloride is the end product of the chlorination procedure. It is a light brown, viscous liquid with

a random of 74.88% and TLC (SiO_2, CH_3OH: CH_2Cl_2 = 1: 1 v/v, R_f = 0.69). The *p-t*-butylcalix[6]arene ethylesteramide, also known as the BEAC6ND4 ionophore, is the end product of the amidation reaction. It is a white solid with a randomness of 65.30%, a melting point of 345-347°C, and TLC (SiO_2, CH_3OH: CH_2Cl_2 = 1: 1 v/v, R_f = 0.79).

Author Contributions

Conceptualization, N.D.; methodology, N.D.; software, A.C.; validation, A.C., H.A.M.A., and S.A.A.P.S.; formal analysis, N.D.; investigation, N.D.; resources, A.C., and A.C.; data curation, H.A.M.A.; writing—original draft preparation, N.D.; writing—review and editing, N.D.; visualization, N.D.; supervision, N.D.; project administration, S.A.A.P.S.; funding acquisition, A.C., and A.C. All authors have read and agreed to the published version of the manuscript.

Institutional Review Board Statement

The authors declare not applicable.

Informed Consent Statement

The authors declare not applicable.

Data Availability Statement

The authors declare that data supporting the findings of this study are available upon reasonable request from the corresponding author.

Funding

This research received no external funding.

Acknowledgments

The authors declare no acknowledgments.

Conflicts of Interest

The authors declare no conflict of interest.

References

1. Arnaud-Neu, F.; Barrett, G.; Corry, D.; Cremin, S.; Ferguson, G.; F. Gallagher, J.; J. Harris, S.; Anthony McKervey, M.; Schwing-Weill, M.J. Cation complexation by chemically modified calixarenes. Part 10. Thioamide derivatives of p-tert-butylcalix[4]-, [5]- and [6]-arenes with selectivity for copper, silver, cadmium and lead. X-Ray molecular structures of calix[4]arene thioamide–lead(II) and calix[4]arene amide–copper(II) complexes. *J. Chem. Soc., Perkin Trans. 2* **1997**, 575-580, https://doi.org/10.1039/A605417J.
2. Kadir, A.N. Selectivity Transport Calixarene and Calixarene Carboxylic to Fe^{3+} of the Mixture Fe, Ni, and Cr Through the Bulk Liquid Membrane 1,2-dichloroethane. *dr. Aloei Saboe* **2014**, *1*, 1-6.
3. Dali, N.; Wahab, A.W.; Firdaus, F.; Maming, M. Synthesis of 5,11,17,23,29,35-hexa(*p-tert*-butyl)-37,39,41-tri(ethoxycarbonylmethoxy)-38,40,42-tri(hydroxy)calix[6]arene from *p-tert*-butylcalix[6]arene. *Sains JKPK* **2012**, *1*, 110-115, https://doi.org/

4. Dali, N.; Wahab, A.W.; Firdaus, F.; Maming, M. Synthesis of Hexa-(*p-tert*-butil)hexa(ethylester)calix[6]-arene from *p-tert*-Butylcalix[6]arene. *Al-Kimia JPSK* **2015**, *3*, 103-109, https://doi.org/10.24252/al-kimia.v3i1.1665.
5. Dali, N.; Wahab, A.W.; Firdaus, F.; Maming, M. Synthesis of 5,11,17,23-tetrakis(*p-tert*-butyl)-25,26,27,28-tetrakis(ethoxycarbonylmethoxy)calix[4]arene from *p-tert*-butylcalix-[4]arene. *dr. Aloei Saboe* **2015**, *2*, 7-12, https://doi.org/
6. Kusumaningsih, T.; Jumina, J.; Siswanta, D.; Mustofa, M. Synthesis of Tetra-*p*-Propenyltetraestercalix[4]-arene and Tetra-*p*-Propenyl tetra carboxylicacidcalix[4]arene from *p-t*-Butylphenol. *Indo. J. Chem.* **2010**, *10*, 122-126, https://doi.org/10.22146/ijc.21491.
7. Arora, V.; Chawla, H.M.; Singh, S.P. Calixarenes as sensor materials for recognition and separation of metal ions. *Arkivoc* **2007**, 172-200.
8. Dali, N.; Dali, S.; Chairunnas, A.; Amalia, H.A.M.; Puspitasari, S.A.A. Synthesis of the BETAC4ND5 ionophore from p-t-butylcalix[4]arene ethylesteramide. *AIP Conf. Proc.* **2022**, *2638*, 060005, https://doi.org/10.1063/5.0104714.
9. Dali, N.; Dali, A.; Dali, S. Synthesis of the BCAC4ND2 Ionophore from *p-t*-Butylcalix[4]-arene Ethylester. *Akta Kimindo* **2020**, *5*, 33-42, http://doi.org/10.12962/j25493736.v5i1.6711.
10. Dali, N.; Wahab, A.W.; Firdaus; Maming; Nurdin, M. Synthesis of Hexa(*p-tert*-butyl)-hexa(carboxylic acid)calix[6]arene from Hexa(*p-tert*-butyl)-hexa(ethyl-ester)calix[6]arene. *Int. J. ChemTech Res.* **2016**, *9*, 486-490.
11. Dali, N.; Dali, A.; Dali, S.; Amalia, H.A.M. Synthesis of the BEAC4ND4 Ionophore from p-t-Butylcalix[4]arene Carboxylic Acid. *Jurnal Kimia Sains dan Aplikasi* **2020**, *23*, 424-431, https://doi.org/10.14710/jksa.23.12.424-431.
12. Dali, N. Synthesis, Characterization, and Application of Derivatives Compound of the Thioamide p-tert-Butylcalix[4]-and-[6]arene as Ionophores on Ion Selective Electrode (ISE) Coated Wire Type for Heavy Metal Content Analysis Hg(II) and Au(I). Level of Dissertation. Graduate School of Hasanuddin University, Makassar, 26 October **2016**.
13. Hisamatsu, Y.; Higuchi, T.; Umezawa, N. Highly stable host-guest complexation of 4-aminoquinoline-based tweezer-type host molecule with chlorin e6. *J. Incl. Phenom. Macrocycl. Chem.* **2025**, *105*, 421-431, https://doi.org/10.1007/s10847-025-01295-z.
14. Chemical Book of Acetyl chloride. Available online: https://www.chemicalbook.com/ChemicalProductProperty_EN_CB4485487.htm (accessed on 15 July **2024**).
15. Wojaczyńska, E.; Ostrowska, M.; Lower, M.; Czyżyk, N.; Jakieła, A.; Marra, A. Recent Advances in Synthesis and Applications of Calixarene Derivatives Endowed with Anticancer Activity. *Molecules* **2024**, *29*, 4240, https://doi.org/10.3390/molecules29174240.
16. Inam, M.; Sareh Sadat, M.-F.; Chen, W. Cyclodextrin Based Host-Guest Inclusion Complex, an Approach to Enhancing the Physicochemical and Biopharmaceutical Application of Poorly Water-soluble Drugs. *Chem. Res. Chin. Univ.* **2023**, *39*, 857-861, https://doi.org/10.1007/s40242-023-3204-0.
17. Hashikawa, Y.; Okamoto, S.; Murata, Y. Synthesis of inter-[60]fullerene conjugates with inherent chirality. *Nat. Commun.* **2024**, *15*, 514, https://doi.org/10.1038/s41467-024-44834-x.
18. Guo, X.-Q.; Yu, P.; Zhou, L.-P.; Hu, S.-J.; Duan, X.-F.; Cai, L.-X.; Bao, L.; Lu, X.; Sun, Q.-F. Low-symmetry coordination cages enable recognition specificity and selective enrichment of higher fullerene isomers. *Nat. Synth.* **2025**, *4*, 359-369, https://doi.org/10.1038/s44160-024-00697-0.
19. Gao, Y.; Guo, J.; Lai, Y.; Lin, J.; Liu, J.; Ji, J.; Yin, P.; Wang, W.; Zhao, H.; Chen, G.; Wang, L.; Fang, X. Polyoxometalate–Organic Hybrid "Calixarenes" as Supramolecular Hosts. *Angew. Chem. Int. Ed.* **2024**, *63*, e202315691, https://doi.org/10.1002/anie.202315691.
20. Kemp, W. Organic Spectroscopy, 3rd Edition; Red Globe Press London: London, United Kingdom, **1991**; https://doi.org/10.1007/978-1-349-15203-2.
21. Lambert, J.B.; Gronert, S.; Shurvell, H.F.; Lightner, D.; Cooks, R.G. Organic Structural Spectroscopy, 2nd Edition; Pearson, **2010**.
22. Sastrohamidjojo, H. Nuclear Magnetic Resonance Spectroscopy. 1st ed.; Liberty: Yogyakarta, Indonesia, **1994**; pp. 21-120.
23. Yang, Y.; Arora, G.; Fernandez, F.A.; Crawford, J.D. Lower-rim versus Upper-rim Functionalization in Diionizable Calix[4]arene-crown-5 Isomers. Synthesis and Divalent Metal Ion Extraction. *Tetrahedron*. **2011**, *67*, 1389-1397, https://doi.org/10.1016/j.tet.2010.12.006

24. Dali, N.; Dali, S.; Chairunnas, A.; Amalia, H.A.M.; Puspitasari, S.A.A. Synthesis of Ionophore from p-t-Butyl-(carboxymethoxy)calix[4]arene Substituted Amide. *Molekul* **2023**, *18*, 50-58, https://doi.org/10.20884/1.jm.2023.18.1.5927.
25. Wu, J.; Gao, J.; Chen, S.-B.; Chung, T.-S. Solvent-activated thin-film nanocomposite membranes molecularly tuned with macrocyclic cavities for efficient water desalination and boron removal. *Chem. Eng. J.* **2023**, *469*, 143982, https://doi.org/10.1016/j.cej.2023.143982.
26. Beshahwored, S.S.; Wang, Y.-T.; Hu, C.-C.; Chung, T.-S. Mixed-charged polyamide-4-sulfocalix [4] arene hollow fiber nanofiltration membranes for heavy metal removal under various pH. *J. Membr. Sci.* **2024**, *705*, 122846, https://doi.org/10.1016/j.memsci.2024.122846.
27. Yang, C.-C.; Chen, P.-C.; Liu, Y.-L. Employing 4-sulfocalix[4]arene in modification of poly(vinyl alcohol) membranes for increasing their permeation fluxes in pervaporation desalination. *J. Membr. Sci.* **2025**, *717*, 123610, https://doi.org/10.1016/j.memsci.2024.123610.
28. Deng, M.; Wei, J.; Qin, Z.; Yan, Z.; Zhang, Z.; Zheng, J.; Yang, L.; Yao, L.; Jiang, W.; Ma, X.; Dai, Z. Incorporating organic macrocyclic cavitands into polyimide to fabricate high-performance hybrid carbon molecular sieve membranes for gas separation. *Sep. Purif. Technol.* **2025**, *362*, 131810, https://doi.org/10.1016/j.seppur.2025.131810.
29. Zhang, X.-Y.; Zhu, D.; Cao, R.-F.; Huo, Y.-X.; Ding, T.-M.; Chen, Z.-M. Enantioselective synthesis of inherently chiral sulfur-containing calix[4]arenes via chiral sulfide catalyzed desymmetrizing aromatic sulfenylation. *Nat. Commun.* **2024**, *15*, 9929, https://doi.org/10.1038/s41467-024-54380-1.
30. Farber, M.; Rawat, V.; Diskin-Posner, Y.; Dobrovetsky, R.; Vigalok, A. Polyaromatic Calixarene Hosts: Calix[4]pyrenes. *Org. Lett.* **2024**, *26*, 5731-5735, https://doi.org/10.1021/acs.orglett.4c01850.
31. Oleksandr, A.Y.; Oleksandr, O.T.; Yevgen, A.K.; Vitaly, I.K. Regioselective Functionalization of the *para*-Positions at the Calix[4]arene Upper Rim. *Curr. Org. Chem.* **2023**, *27*, 510-525, https://doi.org/10.2174/1385272827666230524120812.
32. Rawat, V.; Baheti, A.; Tiwari, O.S.; Vigalok, A. Carbazole-fused calixarene cavities: single and mixed AIEgen systems for NO detection. *Chem. Commun.* **2023**, *59*, 5543-5546, https://doi.org/10.1039/D3CC01181J.
33. Farber, M.; Maity, P.; Baheti, A.; Golombek, A.; Schwartz, T.; Dobrovetsky, R.; Vigalok, A. Long Range Electronic Effects on the Host–Guest Complexation within the Oxygen Depleted 5,5′-Bicalixarene Cavities. *J. Org. Chem.* **2023**, *88*, 15983-15988, https://doi.org/10.1021/acs.joc.3c01566.
34. Li, M.; Zhou, Y.; Wei, B.; Wei, Q.; Yuan, K.; Zhao, Y. Insight into the interaction of host–guest structures for pyrrole-based metal compounds and C_{70}. *J. Chem. Phys.* **2024**, *160*, 124307, https://doi.org/10.1063/5.0195505.
35. Han, X.-N.; Han, Y.; Chen, C.-F. Fluorescent Macrocyclic Arenes: Synthesis and Applications. *Angew. Chem. Int. Ed.* **2025**, *64*, e202424276, https://doi.org/10.1002/anie.202424276.
36. Lhoták, P. Upper rim-bridged calixarenes. *RSC Adv.* **2024**, *14*, 23303-23321, https://doi.org/10.1039/D4RA04663C.

Publisher's Note & Disclaimer